In vivo endothelial siRNA delivery using polymeric nanoparticles with low molecular weight

James E. Dahlman[#1,2,3], **Carmen Barnes**[#4], **Omar Khan**[2,5], **Aude Thiriot**[6], **Siddharth Jhunjunwala**[2], **Taylor E. Shaw**[2], **Yiping Xing**[2], **Hendrik B. Sager**[7], **Gaurav Sahay**[2], **Lauren Speciner**[4], **Andrew Bader**[2], **Roman L. Bogorad**[2], **Hao Yin**[2], **Tim Racie**[4], **Yizhou Dong**[2], **Shan Jiang**[2], **Danielle Seedorf**[2], **Apeksha Dave**[2], **Kamaljeet S. Sandu**[2], **Matthew J. Webber**[2], **Tatiana Novobrantseva**[4], **Vera M. Ruda**[2], **Abigail K.R. Lytton-Jean**[2], **Christopher G. Levins**[2], **Brian Kalish**[8], **Dayna K. Mudge**[8], **Mario Perez**[9], **Ludmila Abezgauz**[10], **Partha Dutta**[7], **Lynelle Smith**[9], **Klaus Charisse**[4], **Mark W. Kieran**[6], **Kevin Fitzgerald**[4], **Matthias Nahrendorf**[7], **Dganit Danino**[10], **Rubin M. Tuder**[9], **Ulrich H. von Andrian**[6], **Akin Akinc**[4], **Avi Schroeder**[11], **Dipak Panigrahy**[6], **Victor Kotelianski**[2], **Robert Langer**[1,2,3,5], and **Daniel G. Anderson**[1,2,3,5]

[1]Harvard-MIT Division of Health Sciences and Technology, Massachusetts Institute of Technology, Cambridge, Massachusetts 02139, USA

[2]David H. Koch Institute for Integrative Cancer Research, Massachusetts Institute of Technology, Cambridge, Massachusetts 02139, USA

[3]Institute for Medical Engineering and Science, Massachusetts Institute of Technology, Cambridge, Massachusetts 02139, USA

[4]Alnylam Pharmaceuticals, Cambridge, Massachusetts 02139, USA

[5]Department of Chemical Engineering, Massachusetts Institute of Technology, Cambridge, Massachusetts 02139, USA

[6]Department of Microbiology and Immunology, Harvard Medical School, Boston 02115, USA

[7]Center for Systems Biology, Massachusetts General Hospital and Harvard Medical School, Boston 02114, USA

[8]Vascular Biology Program, Children's Hospital Boston, and Division of Pediatric Oncology, Dana Farber Cancer Institute, Harvard Medical School, Boston 02115, USA

[9]Program in Translational Lung Research, Division of Pulmonary Sciences and Critical Care Program, Department of Medicine, University of Colorado School of Medicine, Aurora, USA

[10]Deparment of Biotechnology and Food Engineering, and The Russell Berrie Nanotechnology Institute, Technion Israel Institute of Technology, Haifa 3200, Israel

[11]Department of Chemical Engineering, Technion Israel Institute of Technology, Haifa 32000, Israel

[#] These authors contributed equally to this work.

Abstract

Dysfunctional endothelium contributes to more disease than any other tissue in the body. Small interfering RNAs (siRNAs) have the potential to help study and treat endothelial cells *in vivo* by durably silencing multiple genes simultaneously, but efficient siRNA delivery has so far remained challenging. Here we show that polymeric nanoparticles made of low molecular weight polyamines and lipids can deliver siRNA to endothelial cells with high efficiency, thereby facilitating the simultaneous silencing of multiple endothelial genes *in vivo*. Unlike lipid or lipid-like nanoparticles, this formulation does not significantly reduce gene expression in hepatocytes or immune cells even at the dosage necessary for endothelial gene silencing. It mediates the most durable non-liver silencing reported to date, and facilitates the delivery of siRNAs that modify endothelial function in mouse models of vascular permeability, emphysema, primary tumour growth, and metastasis. We believe these nanoparticles improve the ability to study endothelial gene function *in vivo*, and may be used to treat diseases caused by vascular dysfunction.

The vascular system releases factors into the bloodstream, changes the expression of specific receptors, modifies intercellular junctions, and regulates the immune response[1]. Endothelial cells also mediate biological functions including endocytosis and metabolism[2]. Because these processes relate fundamentally to physiology, dysfunctional endothelium promotes more disease than any other tissue in the body[3]. Yet modulating the behavior of endothelial cells *in vivo* remains challenging, particularly in cases which require inhibition of multiple endothelial genes.

RNAi-mediated modification of gene expression has the potential to improve disease treatment and *in vivo* studies of complex biological processes. However its utility is limited by inefficient systemic delivery, with the exception of ionizable lipids and lipid-like compounds termed lipidoids, which reduce hepatic gene expression by 50% after injections of 0.01 mg/kg siRNA[4-7]. By contrast, efficient endothelial gene silencing without the transfection of hepatocytes has remained challenging. While cationic lipids have been reported to deliver siRNA to endothelial cells, these endothelial delivery systems require cumulative doses of up to 7.5 mg/kg to achieve robust gene silencing[8-13].

Nanoformulations based on polymeric materials have delivered siRNA to hepatocytes and melanoma[14,15]. Unlike lipid-based nanoparticles, polymer-nucleic acid nanoparticles condense via multivalent interactions, leading to significantly different physical stability. One polymer class that has been investigated as a gene delivery material is polyethyleneimine (PEI)[16]. Although nanoparticles made from high molecular weight PEI (M_w~25,000 Da) have delivered nucleic acids, they are associated with off-target effects[17]. In contrast, nanoformualtions from low molecular weight PEI (M_w~600 Da) are relatively well tolerated but cannot facilitate siRNA delivery[17,18].

Here we report an siRNA-nanoparticle formulation that reduces endothelial gene expression by over 90% at a dose of 0.10 mg/kg, and by 50% at doses as low as 0.02 mg/kg. This formulation, termed 7C1, differs from traditional lipid-based nanoparticle formulations by delivering siRNA to lung endothelial cells without substantially reducing gene expression in pulmonary immune cells, hepatocytes, or peritoneal immune cells, at low doses. To demonstrate that 7C1-mediated endothelial gene silencing affected function *in vivo*, it was used to modify models of vascular permeability, emphysema, lung tumour growth, and lung metastasis. To our knowledge, these results describe the first highly efficient endothelial RNA delivery system, as well as the first description of *in vivo* endothelial multigene silencing, and suggest that 7C1 may have utility for the study and treatment of vascular disease *in vivo*.

Efficient siRNA delivery to endothelium *in vitro* and *in vivo*

A diverse library of epoxide-modified lipid-polymer hybrids was synthesized (Supplementary Information, Fig. 1a, Supplementary Fig. 1a). Compounds were tested for their ability to reduce gene expression in HeLa cells at four different lipid: siRNA mass ratios (2.5:1, 5:1, 10:1, 15:1) (Supplementary Fig. 1b). HeLa cells expressing Firefly and Renilla luciferase were chosen as a first-pass screen for these 2,000 nanoparticles formulated with siLuciferase because of the cost-effectiveness of the assay[5]. We defined a successful nanoparticle as one that silenced Firefly luminescence more than 70%, but decreased Renilla luminescence less than 25%. While only 0.9% percent of the library was successful at a mass ratio equal to 2.5, 6.5% were successful when the mass ratio equaled 15 (Table 1). We then measured Firefly luminescence as a function of lipids bound to successful PEI_{600} compounds. Luminescence decreased with the number of lipids bound (Supplementary Fig. 1c). A subset of formulations tested in HeLa cells were tested for their ability to deliver siRNA to human (HMVEC) and murine (bEnd.3) endothelial cells *in vitro*. The most effective compound, termed 7C1 based on its composition, reduced target mRNA expression by more than 85% in HeLa, HMVECs, and bEnd.3 cells at a dose of 30 nM (Fig. 1b). Interestingly, 7C1 efficacy did not change with mass ratio in HeLa cells (Supplementary Fig. 1d). Only 2 nM was required to reduce target gene expression in bEnd.3 cells by 50%, and 7C1 did not affect bEnd.3 cell morphology or induce apoptosis *in vitro* at doses as high as 133 nM (Supplementary Fig. 1e-f).

7C1 was synthesized by reacting C_{15} epoxide-terminated lipids with PEI_{600} at a 14:1 molar ratio, and was formulated with $C_{14}PEG_{2000}$ to produce nanoparticles with a diameter between 35 and 60 nm that were stable in PBS solution for at least 40 days (Fig. 1c-e, Supplementary Fig. 1g-i). Particles formed multilamellar vesicles rather than periodic aqueous compartments containing siRNA that make up stable nucleic acid lipid particle formulations[19] (Fig. 1d, Supplementary Fig. 1j). Because particle charge at different pH can affect delivery by modifying interactions with serum proteins, the zeta potential of 7C1 formulated with siRNA at blood physiological pH (7.4) and pKa were measured[6] (Fig. 1f). While 7C1 formed electrically neutral particles at pH 7.4, its pKa was 5.0. Interestingly, this value contrasts the pKa of particles optimized for hepatocyte delivery[20].

We investigated the serum kinetics and biodistribution of 7C1 siRNA nanoparticles *in vivo*. 7C1 was complexed with Alexa647-tagged siRNA and injected intravenously. After one hour, skin tissue whole-mounted for confocal microscopy showed colocalization between 7C1 and endothelial cells, suggesting endothelial cells endocytosed 7C1 *in vivo* (Fig 1g). Endothelial cell uptake was confirmed by an increase in Alexa647 mean fluorescence intensity in endothelial cells sorted from pulmonary tissue one hour after injection with 7C1 formulated with Alexa647-tagged siRNA (Fig. 2g). 7C1 serum kinetics was then measured. 7C1 serum concentration decreased by 50% within 20 minutes after intravenous injection, indicating the formulation was rapidly cleared or endocytosed (Fig. 1h). To investigate 7C1 biodistribution, Cy5.5 fluorescence was quantified 4 and 24 hours after injection (when 7C1 serum concentrations were negligible) (Fig. 1i). Renal fluorescence was high, indicating that the kidneys aid in the clearance of siRNA delivered by 7C1. *In vitro*, HMVECs take up 7C1 via caveolae- and clathrin-mediated endocytosis (Supplementary Information, Fig. 2a).

To confirm endothelial localization resulted in functional siRNA delivery, gene silencing was measured after 7C1 was formulated with siRNAs targeting genes expressed primarily by endothelial cells. 7C1 was formulated with siRNA targeting the gene ICAM-2 and injected with a dose of 0.6 mg/kg on day one and four. Five days later, skin was analyzed with confocal microscopy and flow cytometry (Supplementary Fig. 2a-b). ICAM-2 expression on lymph node and omentum endothelial cells was also measured with flow cytometry (Supplementary Fig. 2b). ICAM-2 expression decreased compared to PBS- and siLuciferase- (termed siCntrol) treated mice. 7C1 was then formulated with 0.60, 0.05, 0.02, or 0.007 mg/kg si-ICAM2 and injected once (Fig. 2b). Because ICAM-2 is principally expressed by endothelial cells in all major tissue beds, this assay detect endothelial gene silencing in any organ[21]. 7C1 reduced ICAM-2 mRNA expression in the pulmonary, cardiovascular, and renal endothelium by 50% after a dose of 0.02, 0.08, and 0.08 mg/kg, respectively (Fig. 2b). To ensure efficient delivery was not limited to siICAM-2, we measured gene silencing in mice treated with siRNA targeting VE-cadherin (VEcad), a junctional protein whose expression is limited to endothelium. Cardiovascular, renal, and pulmonary VEcad mRNA decreased by 50% at doses of 0.04, 0.08, and less than 0.02 mg/kg, respectively (Fig. 2c). 7C1-siVEcad also reduced VEcad protein levels in whole lung homogenates at 0.03 mg/kg (Fig. 2d). We then investigated whether reduced VEcad protein levels increased vascular permeability. Compared to mice treated with PBS or siCntrol, the extravasation of Evans Blue Dye out of the pulmonary vasculature increased 2.5 fold seven and fourteen days after a single 0.6 mg/kg injection of siVEcad (Fig. 2e). These data demonstrate that 7C1 facilitates the most efficient non-liver siRNA delivery reported to date.

Because *in vivo* multigene silencing requires highly efficient delivery, it has been limited to hepatocytes[5]. 7C1 silenced five endothelial genes (Tie1, Tie2, VEcad, VEGFR-2, and ICAM2) concurrently. Three days following an intravenous injection with a total dose of 0.25 mg/kg, target mRNA of all five genes decreased between 60% and 80% in pulmonary vasculature (Fig. 2f, Supplementary Fig. 2c-e). Target gene expression remained constant after siCntrol was injected with a total dose of 2.0 mg/kg, suggesting reduced mRNA levels were due to RNAi. To our knowledge, this is the first demonstration of multi-gene silencing in endothelial cells *in vivo*.

Efficient delivery also facilitates durable gene silencing, since the duration of gene silencing is generally dose dependent[5]. mRNA silencing was measured as a function of time after a 0.6 mg/kg injection of siICAM-2 (Fig. 2g). Pulmonary ICAM-2 mRNA expression initially decreased by 92% and remained suppressed between 73% and 85% for twenty-one days. By contrast, cardiovascular and renal endothelial ICAM-2 expression continually increased over the first twenty-eight days, reaching 50% of initial expression after day ten, again suggesting less efficient endothelial cell delivery in these vascular beds compared to lung endothelium (Fig. 2g). We then measured gene silencing in different organs after modifying particle size and 7C1: siRNA mass ratio (Supplementary Information, Supplementary Fig. 2f-i). 7C1 was complexed siRNA targeting the endothelial specific gene Tie2[21]. In all cases, the most potent delivery was measured in pulmonary endothelial cells (Supplementary Fig. 2f-i).

While others have reported siRNA delivery to the lung, functional gene silencing required doses much higher than 0.02 mg/kg. Since the relative silencing in different cell types informs the type of *in vivo* models nanoparticles can be used to study, we studied 7C1 biodistribution and silencing in pulmonary epithelial cells, hematopoietic cells, T cells, and B cells (Fig. 3a-c). We also measured gene silencing in hepatocytes and peritoneal immune cells, two cell types that have been preferentially transfected by lipid nanoparticles (Fig. 3d-f).

We quantified uptake of Alexa647 labeled siRNA delivered by 7C1. One hour after a 1.0 mg/kg injection, lungs were digested into a single cell suspension and labeled with antibodies. Flow cytometry revealed that Alexa647 median fluorescent intensity was significantly higher in endothelial cells than pulmonary epithelial cells, hematopoietic cells, T cells, and B cells (Fig. 3a). Twenty-four hours after injection, endothelial cell uptake decreased. While the significance of the decreased signal is unknown, it could result from fluorophore cleavage. We then used flow cytometry to simultaneously quantify ICAM-2 protein expression in pulmonary endothelial cells, hematopoietic cells, T cells, and B cells. Three days following injection of 0.30, 0.20, 0.10, or 0.05 mg/kg, pulmonary endothelial cell ICAM-2 median fluorescent intensity decreased between 60% and 68% compared to cells from siCntrol treated mice (Fig. 3b). ICAM-2 median fluorescent intensity did not decrease in pulmonary hematopoietic cells, T cells, or B cells. The relative delivery to lung endothelium and epithelium was then quantified with siRNA targeting Integrinß1 (Fig. 3c). Two days after injection, lungs were digested before epithelial and endothelial cells were sorted into separate tubes with fluorescence activated cell sorting. The purity of the sorted cells was confirmed by measuring cell-specific markers using RT-PCR (Supplementary Fig. 2j). Compared to siCntrol-treated cells, endothelial cell Integrinß1 mRNA decreased between 70% and 82%, while epithelial cell mRNA did not change substantially (Fig. 3c). These data indicate that at these doses, 7C1 preferentially delivers siRNA to pulmonary endothelial cells.

We then analyzed whether 7C1 delivered siRNA to hepatocytes, which are preferentially targeted by many lipid nanoparticle formulations (Fig. 3d). We measured the expression of a hepatocyte-specific gene Factor 7 (F7) after injection with the highly potent siF7[5]. While F7 serum concentration remained constant after siF7 was injected at a dose of 1.5 mg/kg, and was only reduced by 35% after an injection of 2.0 mg/kg, the positive control lipid

nanoparticle Hepat01 decreased F7 expression by 95% after a 0.30 mg/kg dose (Fig. 3d). To confirm that 7C1 reduced endothelial gene silencing without silencing hepatocyte gene expression, 7C1 was simultaneously complexed with siF7 and siTie2 (Fig. 3e). Since efficacy can vary with the molar ratio of PEG and cholesterol, we performed this two-gene experiment with particles formulated with different 7C1: Cholesterol: $C_{14}PEG_{2000}$ molar ratios. Two formulations reduced lung Tie2 mRNA by nearly 90% after a single 0.15 mg/kg dose, but did not reduce F7 expression (Fig. 3e).

Intravenously injected particles may also transfect peritoneal immune cells, especially CD11b^{+} monocytes and macrophages[22]. CD45 median fluorescent intensity was quantified in immune cells isolated from the peritoneal cavity following intravenous injection of 2.0 mg/kg 7C1 formulated with an siRNA targeting CD45 (siCD45)[22] (Fig. 3f). CD45 protein expression remained constant in macrophages, B cells, T cells, and dendritic cells following treatment with 7C1 (Fig. 3f). By contrast, CD45 expression decreased in macrophages cells following treatment with the positive control lipid nanoparticle C12-200. Taken together, these data indicate that 7C1 does not deliver siRNA to hepatocytes or peritoneal immune cells in healthy BL\6 mice at any dose tested.

Endothelial RNAi affects multiple animal models

Whether RNA delivery could change endothelial function was then investigated in mouse models of emphysema, primary tumour growth, and lung metastasis. Emphysema is characterized by decreased pulmonary surface area, which reduces gas transport, causing dyspnea and cough[23,24]. Along with macrophage-mediated protease imbalance, decreased VEGF and VEGFR-2 expression has been documented in lungs of patients with chronic obstructive pulmonary disease; moreover, genetic Cre-lox mediated deletion of VEGF causes emphysema in mice[24]. VEGF receptor blockade with SU5416 promotes emphysema in rodents, leading to decreased alveolar surface to volume ratios, increased lung volume, and increased distance between alveolar walls (termed the mean linear intercept)[23]. Because SU5416 simultaneously inhibits VEGFR-1 and VEGFR-2, we characterized pulmonary phenotype following VEGFR-2 specific silencing. VEGFR-2 silencing induced emphysema-like changes, indicated by decreased alveolar surface to volume ratios and increases in lung volume and mean linear intercept compared to siCntrol treated mice (Fig. 3g-i, Fig. 3k). These changes were not due to infiltration of myeloid cells (Fig. 3j). These results suggest VEGFR-2 specific silencing is sufficient to induce emphysema-like phenotypes in mice, and that systemic endothelial cell RNAi can be used to investigate the role of endothelial gene function *in vivo*.

The therapeutic effect of endothelial RNAi on primary tumour growth was then investigated in a Lewis lung carcinoma model. Previous work demonstrated antibodies targeting VEGFR-1 and Dll4 can reduce primary tumour growth through disrupted or non-productive angiogenesis, respectively[25,26]. In particular, targeting VEGFR-1, which is expressed on endothelial cells and pro-angiogenic myeloid cells, reduced tumour progression, metastasis, and formation of a pre-metastatic niche[27,28]. However, monoclonal antibodies may function differently than RNAi-based methods, which inhibit both extracellular and intracellular signaling[29]. To investigate whether therapeutic deletion of VEGFR-1 and Dll4, both of

which have intracellular signaling components, would have similar effects as therapeutic antibodies, 7C1 was complexed with siCntrol, siVEGFR-1, or siDll4. Compared to siCntrol, siVEGFR-1 and siDll4 formulations had a significant therapeutic effect, reducing primary tumour growth by 40% and 70%, respectively, and increasing tumour necrosis (Fig. 4a-c). While some tumours treated with siVEGFR-1 exhibited high levels of cell death, others showed low levels[30]. These data suggest targeted deletion of both the intracellular and extracellular portion of VEGFR-1 or Dll4 may reduce primary tumour growth.

While the role of VEGFR-1 and Dll4 in primary tumour growth has been extensively studied, the role of these genes, particularly Dll4, in metastasis is less clearly understood[31,32]. Consequently, the effect of VEGFR-1 and Dll4 deletion on lung tumour metastases was studied in a metastatic Lewis lung carcinoma model (Fig. 4d-e, Supplementary Fig. 3). siVEGFR-1 reduced surface metastases by 52%, while siDll4 reduced surface metastases by 63% compared to siCntrol treated mice (Fig. 4d-e). Lung weight, which correlates to the growth of lung metastases, decreased by 50% after siVEGFR-1 therapy and 60% after siDll4 therapy (Supplementary Fig. 3).

7C1 *in vivo* tolerability

7C1 nanoformulations were well tolerated in animal models of toxicity following acute and chronic high-dose treatment (Supplementary Fig. 4). We measured serum concentration of markers associated with toxicity after four 0.6 mg/kg intravenous injections in highly immunoactive $CD1^+$ mice, a mouse model used for pre-clinical toxicology studies. Mice were injected with a 0.6 mg/kg dose of siCntrol or siICAM-2 once per week for four weeks. Forty-eight hours after the last injection, serum concentration of markers for hepatic, cardiovascular, and renal injury were quantified. Importantly, we observed no evidence of kidney damage (Supplementary Fig. 4a).

7C1 tolerability was also investigated in BL\6 mice at doses much higher than those required for functional gene silencing (2 mg/kg) in acute and chronic models. Over twenty-eight days, mice were injected eight times with PBS solution or 2 mg/kg 7C1. Murine weight gain equaled that of mice injected with PBS (Supplementary Fig. 4b). Four hours after the final injection, mice were sacrificed and lungs were removed before mRNA expression of cytokines (IL-6, TNF-α), markers of endothelial dysfunction (ICAM-2, E-selectin), and immune cell infiltration (CD45) were quantified (Supplementary Fig. 4c). Serum concentration of 30 cytokines was also quantified. mRNA expression and cytokine concentration did not increase significantly when compared to PBS treated mice (Supplementary Fig. 4d).

We then measured serum cytokine concentration two, four, six, and twenty-four hours following a 2.0 mg/kg injection. While the serum concentration of five factors did increase between two and six hours, only one factor (CXCL2) equaled the concentration of mice treated with a low dose LPS control, and all five returned to baseline twenty-four hours after injection (Supplementary Fig. 4e). These data suggest that while 7C1 likely interacts with cells to produce a transient response at doses much higher than those required for gene silencing, the formulation appears to be well tolerated in multiple mouse models *in vivo.*

Conclusion

Motivated by the utility of hepatocyte-targeting vehicles and the role of vasculature in pathologies ranging from heart disease to cancer, we identified a nanoparticle that efficiently delivers siRNA to endothelial cells. Unlike previously reported lipid and lipidoid-based nanoparticles, 7C1 transfected endothelial cells *in vivo* at low doses, without significantly reducing gene expression in hepatocytes, peritoneal immune cells, pulmonary epithelial cells, or pulmonary immune cells. While the molecular mechanism governing this effect remains under investigation, it may be due to interactions with serum proteins, which can promote delivery to certain cell types[33]. As a result, 7C1 may be an interesting system to study how physiochemical interactions between nanomaterials and serum proteins direct nanoparticles to endothelial cells *in vivo*[34].

The potency of this nanoformulation allowed for the simultaneous silencing of multiple endothelial genes. While some immune cells are known to express Tie1, Tie2, and ICAM-2, the lack of significant pulmonary immune cell gene silencing mediated by 7C1 indicates that this multigene silencing occurred primarily in endothelial cells. We anticipate that 7C1 may have utility in the study of gene combinations in complex biological pathways *in vivo*, a strategy termed *in vivo genomics*.

7C1 reduced primary tumour growth and lung metastases in a model of lung cancer. While this study examined targets whose extracellular activity can also be inhibited by antibodies, future therapies may be designed to target combinations of proteins currently considered 'undruggable'. Similarly, future RNA therapies may enhance the effects of non-RNA drugs. For example, modifying the expression of gene involved in the exocytosis of a small molecule might enhance its delivery.

7C1 durably reduced target gene expression in multiple animal models. This ability to extend a therapeutic effect may increase the utility of *in vivo* endothelial RNAi. Because 7C1 is well tolerated at doses far higher than those required for gene silencing, we believe this technology will be used to manipulate gene expression *in vivo*. Our results demonstrate that 7C1 nanoformulations facilitate highly efficient endothelial RNA delivery, providing biologists and engineers with a new tool to deliver siRNA to endothelium.

Supplementary Material

Refer to Web version on PubMed Central for supplementary material.

Acknowledgments

References

1. Pober JS, Sessa WC. Evolving functions of endothelial cells in inflammation. Nat Rev Immunol. 2007; 7:803–815. [PubMed: 17893694]

2. Hagberg CE, et al. Targeting VEGF-B as a novel treatment for insulin resistance and type 2 diabetes. Nature. 2012; 490:426–430. [PubMed: 23023133]

3. Kumar V, Abbas A, Fausto N, Aster J. Robbins and Cotran Pathologic Basis of Disease (Eighth Edition). 2009

4. Kanasty R, Dorkin JR, Vegas A, Anderson D. Delivery materials for siRNA therapeutics. Nat Mater. 2013; 12:967–977. [PubMed: 24150415]

5. Love KT, et al. Lipid-like materials for low-dose, in vivo gene silencing. Proc Natl Acad Sci USA. 2010; 107:1864–1869. [PubMed: 20080679]

6. Semple S, et al. Rational design of cationic lipids for siRNA delivery. Nature biotechnology. 2010; 28:172–176.

7. Whitehead KA, Langer R, Anderson DG. Knocking down barriers: advances in siRNA delivery. Nature Reviews Drug Discovery. 2009; 8:129–138.

8. Aleku M, et al. Atu027, a Liposomal Small Interfering RNA Formulation Targeting Protein Kinase N3, Inhibits Cancer Progression. Cancer research. 2008; 68:9788–9798. [PubMed: 19047158]

9. Aleku M, et al. Intracellular localization of lipoplexed siRNA in vascular endothelial cells of different mouse tissues. Microvascular Research. 2008; 76:31–41. [PubMed: 18455200]

10. Santel A, et al. RNA interference in the mouse vascular endothelium by systemic administration of siRNA-lipoplexes for cancer therapy. Gene Ther. 2006; 13:1360–1370. [PubMed: 16625242]

11. Santel A, et al. A novel siRNA-lipoplex technology for RNA interference in the mouse vascular endothelium. Gene therapy. 2006; 13:1222–1234. [PubMed: 16625243]

12. Polach KJ, et al. Delivery of siRNA to the Mouse Lung via a Functionalized Lipopolyamine. Mol Ther. 2011; 11:210.

13. Kaufmann J, Ahrens K, Santel A. RNA interference for therapy in the vascular endothelium. Microvascular Research. 2010; 80:286–293. [PubMed: 20144624]

14. Davis ME, et al. Evidence of RNAi in humans from systemically administered siRNA via targeted nanoparticles. Nature. 2010:1–8.

15. Rozema DB, et al. Dynamic PolyConjugates for targeted in vivo delivery of siRNA to hepatocytes. Proc Natl Acad Sci US A. 2007; 104:12982–12987.

16. Godbey WT, Wu KK, Mikos AG. Poly(ethylenimine) and its role in gene delivery. Journal of Controlled Release. 1999; 60:149–160. [PubMed: 10425321]

17. Breunig M, Lungwitz U, Liebl R, Goepferich A. Breaking up the correlation between efficacy and toxicity for nonviral gene delivery. Proc Natl Acad Sci U S A. 2007; 104:14454–14459. [PubMed: 17726101]

18. Richards Grayson AC, Doody AM, Putnam D. Biophysical and structural characterization of polyethylenimine-mediated siRNA delivery in vitro. Pharmaceutical research. 2006

19. Crawford R, et al. Analysis of lipid nanoparticles by Cryo-EM for characterizing siRNA delivery vehicles. Int J Pharm. 2011; 403:237–244. [PubMed: 20974237]

20. Jayaraman M, et al. Maximizing the potency of siRNA lipid nanoparticles for hepatic gene silencing in vivo. Angew Chem Int Ed Engl. 2012; 51:8529–8533. [PubMed: 22782619]

21. Huang H, Bhat A, Woodnutt G, Lappe R. Targeting the ANGPT-TIE2 pathway in malignancy. Nat Rev Cancer. 2010; 10:575–585. [PubMed: 20651738]

22. Novobrantseva TI, et al. Systemic RNAi-mediated Gene Silencing in Nonhuman Primate and Rodent Myeloid Cells. Molecular Therapy - Nucleic Acids. 2012

23. Kasahara Y, et al. Inhibition of VEGF receptors causes lung cell apoptosis and emphysema. J Clin Invest. 2000; 106:1311–1319. [PubMed: 11104784]

24. Tuder RM, Yun JH. Vascular endothelial growth factor of the lung: friend or foe. Curr Opin Pharmacol. 2008; 8:255–260. [PubMed: 18468486]

25. Thurston G, Noguera-Troise I, Yancopoulos GD. The Delta paradox: DLL4 blockade leads to more tumour vessels but less tumour growth. Nat Rev Cancer. 2007; 7:327–331. [PubMed: 17457300]

26. Fischer C, Mazzone M, Jonckx B, Carmeliet P. FLT1 and its ligands VEGFB and PlGF: drug targets for anti-angiogenic therapy? Nat Rev Cancer. 2008; 8:942–956. [PubMed: 19029957]

27. Lyden D, et al. Impaired recruitment of bone-marrow-derived endothelial and hematopoietic precursor cells blocks tumor angiogenesis and growth. Nat Med. 2001; 7:1194–1201. [PubMed: 11689883]

28. Kaplan RN, et al. VEGFR1-positive haematopoietic bone marrow progenitors initiate the pre-metastatic niche. Nature. 2005; 438:820–827. [PubMed: 16341007]

29. Tammela T, et al. VEGFR-3 controls tip to stalk conversion at vessel fusion sites by reinforcing Notch signalling. Nat Cell Biol. 2011; 13:1202–1213. [PubMed: 21909098]

30. Stevens JB, et al. Heterogeneity of cell death. Cytogenet Genome Res. 2013; 139:164–173. [PubMed: 23548436]

31. Kuramoto T, et al. Dll4-Fc, an Inhibitor of Dll4-Notch Signaling, Suppresses Liver Metastasis of Small Cell Lung Cancer Cells through the Downregulation of the NF-kappaB Activity. Mol Cancer Ther. 2012; 11:2578–2587. [PubMed: 22989420]

32. Garcia A, Kandel JJ. Notch: a key regulator of tumor angiogenesis and metastasis. Histol Histopathol. 2012; 27:151–156. [PubMed: 22207549]

33. Akinc A, et al. Targeted delivery of RNAi therapeutics with endogenous and exogenous ligand-based mechanisms. Mol Ther. 2010; 18:1357–1364. [PubMed: 20461061]

34. Monopoli MP, Aberg C, Salvati A, Dawson KA. Biomolecular coronas provide the biological identity of nanosized materials. Nat Nanotechnol. 2012; 7:779–786. [PubMed: 23212421]

35. Chen D, et al. Rapid discovery of potent siRNA-containing lipid nanoparticles enabled by controlled microfluidic formulation. J Am Chem Soc. 2012; 134:6948–6951. [PubMed: 22475086]

36. Whitehead K, Dahlman JE, Langer RS, Anderson DG. Silencing or Stimulation? siRNA Delivery and the Immune System. Annual Review of Chemical and Biomolecular Engineering. 2010

37. Panigrahy D, et al. Epoxyeicosanoids stimulate multiorgan metastasis and tumor dormancy escape in mice. J Clin Invest. 2012; 122:178–191. [PubMed: 22182838]
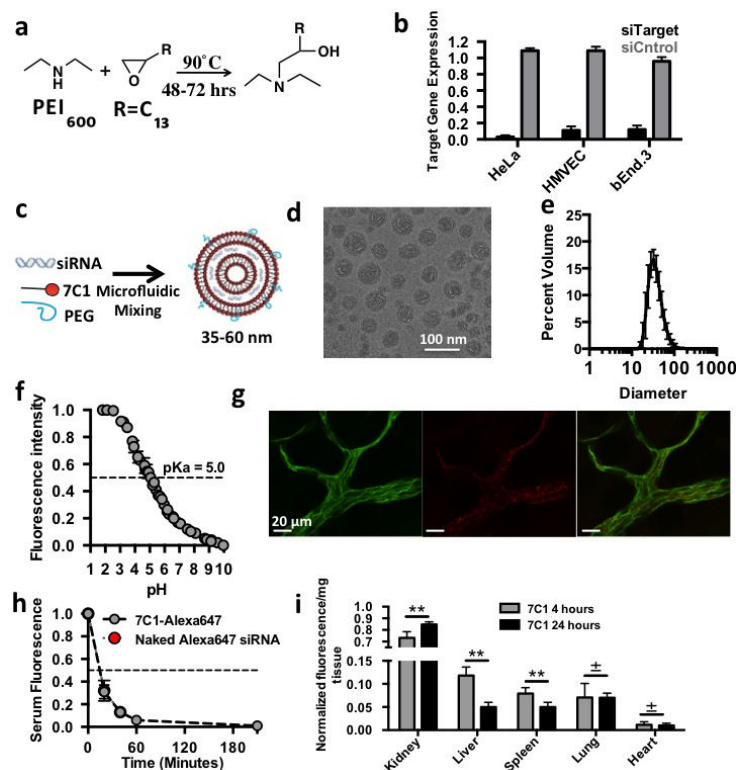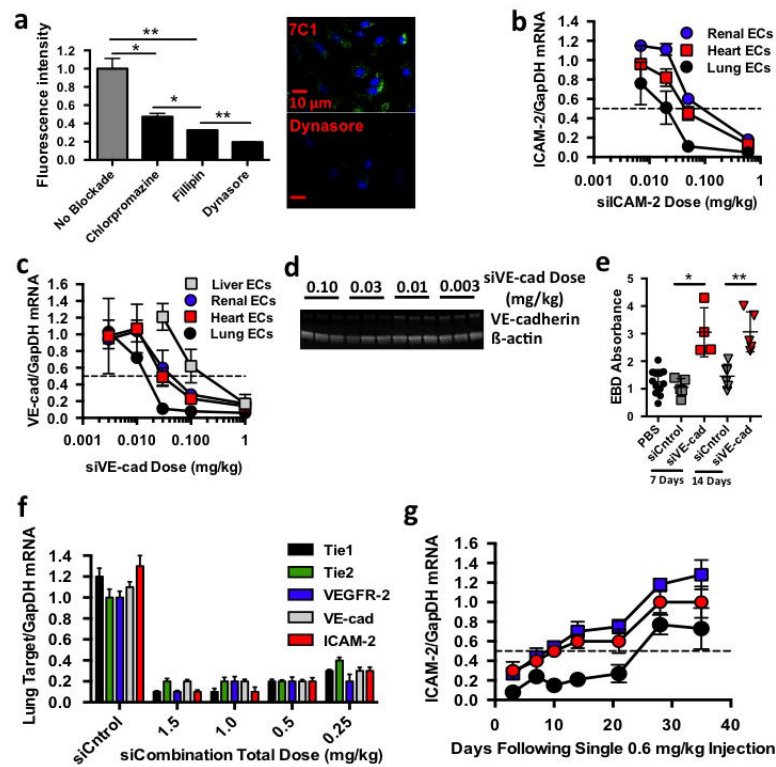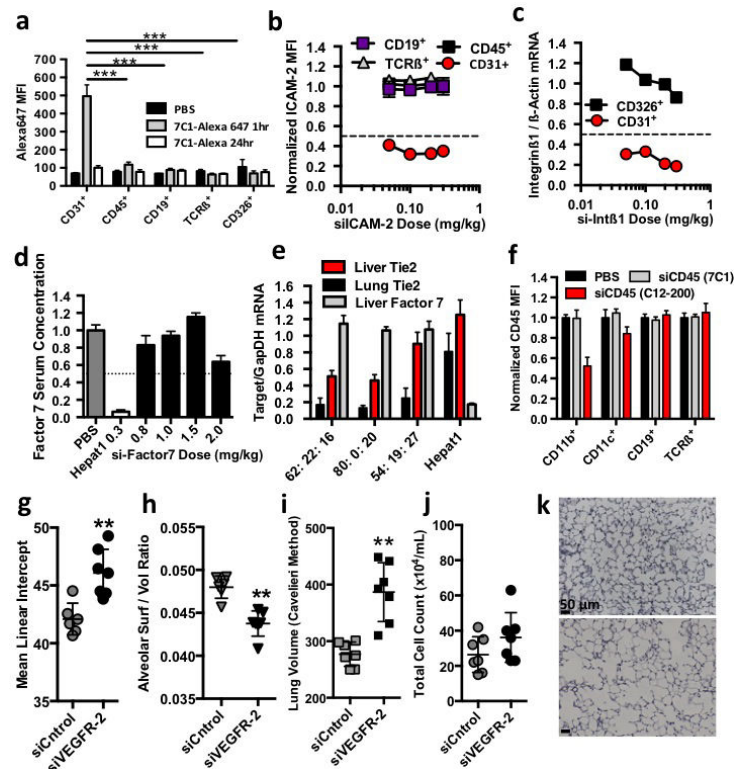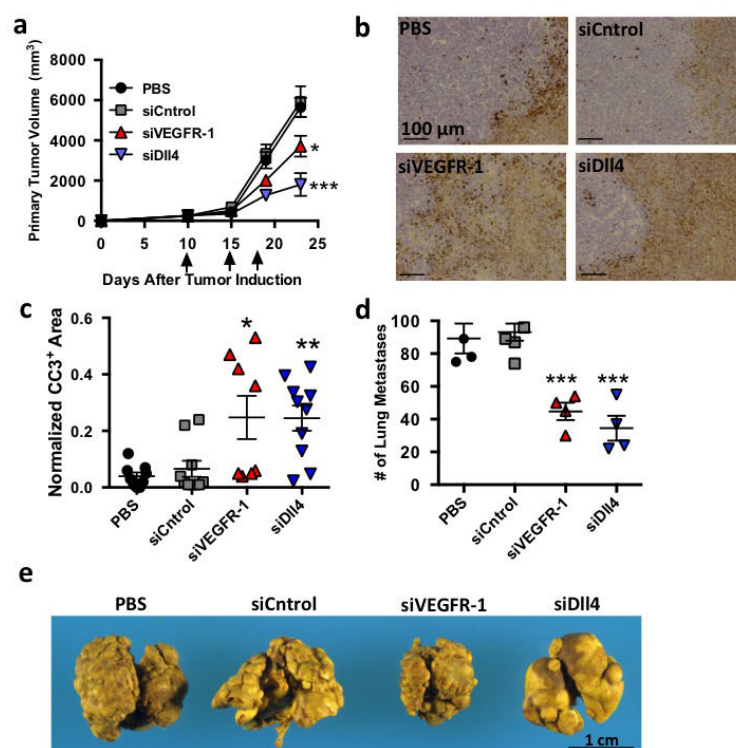
Figure 1.

7C1 synthesis, characteri zation, and *in vivo* biodistribution. (**A**) 7C1 synthesis scheme. (**B**) Target gene expression 24 hours following 30 nM treatment with siRNA in human cervical carcinoma (HeLa), human primary endothelial (HMVEC), and murine endothelial (bEnd.3) cells. HeLa target gene expression was measured as Firefly luminescence in HeLa cells expressing Luciferase that were treated with siRNA targeting luciferase. bEnd.3 and HMVEC target gene expression was measured as Tie2 mRNA levels following treatment with siRNA targeting Tie2. (**C**) 7C1 formulation scheme. 7C1 nanoparticles were mixed with $C_{14}PEG_{2000}$ and siRNA in a high throughput microfluidic chamber as previously described[30]. (**D**) 7C1 internal structure characterized by cryo-TEM. Dark bands indicate lipid layers and light bands indicate regions with siRNA. (**E**) Average 7C1 hydrodynamic diameter, measured by dynamic light scattering, and weighted by volume (N=20 formulations). (**F**) TNS nuorescence of formulated 7C1 nanoparticles as a function of pH (used to measure 7C1 pKa). (**G**) Representative confocal image of Alexa647-tagged siRNA complexed to 7C1 one hour after intravenous injection. CD31 is a ubiquitous marker for endothelium (Scale bar = 20 μm). (**H**) Serum Cy5.5 concentration following with 7C1-Cy5.5 siRNA or naked Cy5.5 siRNA (**I**) Cy5.5 nuorescence/mg tissue after injection with 7C1-Cy5.5 siRNA. Tissues were removed after injection and weighed individually. Cy5.5 intensity was normalized to each individual tissue. Timepoints were selected to measure systemic siRNA accumulation after Cy5.5 was cleared from serum. N=4-S mice/group. In all cases, data shown as mean +/− std. *p<0.05, ** p<0.005, ***p<:0.0008, ±p<0.75.

Figure 2.
7Cl delivers siRNA to endothelial cells. **(A)** Alexa647 fluorescence uptake in HMVEC cells following 7CI-Alexa647 siRNA treatments and administration of small molecules blockading clathrin (Chlorpromazine), caveolin (Fillipin), and both endocytotic pathways (Oynasore). **(B)** ICAM-2/GapDH mRNA ratios (normalized to PBS-treated mice) following intravenous injection of 7Cl-silCAM-2. **(C)** VE-cadherin/GapDH mRNA ratios (normalized to PBS-treated mice) following intravenous injection of 7Cl-siVEcad. **(D)** VE-cadherin and ß-actin protein expression following treatment with 7Cl-siVEcad. **(E)** Evans Blue Dye pulmonary absorbance seven and fourteen days following a 0.6 mg/kg injection of 7Cl-siVEcad. **(F)** Target/GapDH mRNA ratios (normalized to PBS-treated mice) following injection of 7Cl formulated with siCntrol or five siRNAs targeting ICAM-2, Tie2, VE-cadherin, VEGFR2, or Tiel, respectively (siCombination). **(G)** ICAM-2/GapDH mRNA levels as a function of time following a 0.6 mg/kg injection of siICAM-2. Data shown as mean +/− std. N=4 to 5 mice per group, *p< 0.05, ** p< 0.005.

Figure 3.
7Cl preferentially delivers siRNA to pulmonary endothelial cells *in vivo*. **(A)** Alexa647 median fluorescent intensity in pulmonary endothelial (C031[+]), hematopoietic (C045[+]), epithelial (C0326[+]), B (CDI9^{+}), or T (TCRß^{+}) cells isolated from mice after treatment with 7Cl formulated with Alexa647-tagged siRNA. Statistical significance calculated between endothelial cells and other pulmonary cell types one hour after injection. **(B)** ICAM-2 median fluorescent intensity in pulmonary cells (normalized to siCntrol-treated mice) isolated from mice three days followings treatment with 7Cl-silCAM -2. **(C)** Integrinß/ß-actin mRNA ratios (normalized to siCntrol-treated mice) in pulmonary endothelial and epithelial cells isolated from mice two days after treatment with silntegrinßl. **(D)** Factor 7 serum concentration (normalized to PBS-treated animals) two days following treatment with liver targeting molecule HepatOl-siFactor7 or 7Cl-siFactor7 **(E)** Tie2 and Factor7/GapOH mRNA expression following a 0.15 mg/kg injection of 7Cl concurrently formulated with siTie2 and siFactor7. Particles were formulated with different 7Cl: Cholesterol: C14PEGlOOO molar ratios. 7Cl decreased Tie2 mRNA expression in pulmonary, renal, and hepatic endothelium without reducing F7 mRNA expression. **(F)** C045 median fluorescent intensity following treatment with 7Cl-siC04S or positive control CI2-200-siC045. (**G-K**) Mean Linear Intercept (MU) between alveoli, pulmonary surface/volume ratio, total volume, and pulmonary histology following two 0.5 mg/kg injections of siCntrol or siVEGFR2. Increased MLI, alveolar volume, decreased surface/volume ratios, and constant infiltrating myeloid cells are consistent with an induced emphysema-like phenotype (N=6 to 7 animals / group, data shown as average +/− std, scale bar = 50 um)*p < 0.05, **p<0.002, ***p<0.00l.

Figure 4.
7Cl mediated mRNA silencing modifies endothelial function *in vivo*. **(A)** Primary lewis lung Carcinoma (LLC) growth following three 1.0 mg/kg treatments with PBS, siCntrol. siVEGFR-l, or siDII4 (N=7 to 10 animals per group, data shown as average +/− SEM). **(B,C)** Representative image and quantification of cleaved caspase 3 (CC3) staining, a marker for apoptosis, following treatment with PBS, siCntrol, siVEGFR-l, siDlI4. Normalized CC3$^+$ area defined as the total CC3$^+$ surface area divided by the tumor surface area. Scale bar = 100 μm. **(D)** Number of pulmonary surface metastases following four 1.0 mg/kg injections with PBS, siCntrol. siVEGFR-l, or siDli4 (N=4 to 6 per group, data shown as average +/− SEM). To measure effects independent of primary tumor growth, animals were not treated until after primary tumor resection. **(E)** Murine lungs with metastatic lesion removed after treatment with PBS, siluc, siVEGFR-l, or siDlI4 . *p < 0.05, **p<0.002, ***p<0.00l.

Table 1

The percent of compounds reducing Firefly luminescence more than 70% while not reducing Renilla luminescence more than 25% as a function of lipid: siFire mass ratio.

Compound: siFire Mass Ratio	Successful nanoparticles (%)
2.5	0.9
5	0.7
10	3.5
15	6.5

Table 2

Intravenous dose required to reduce target gene mRNA expression by 50% *in vivo* (mg/kg), termed the ED_{50}.

Gene	Lung	Heart	Kidney
VEcad	0.02	0.04	0.08
ICAM2	0.02	0.08	0.15
Tie2	0.04	0.12	0.12
VEGFR-2 [*]	0.05	0.10	0.25
Tie1 [*]	0.05	0.10	0.15

[*] ED_{50} value calculated from multigene silencing experiment (Fig. 2d).

Table 3

Target gene expression in (B) cardiovascular, (C) renal, and (D) hepatic vasculature following injection of 7C1 complexed with siRNA targeting Luc or Tie1, Tie2, VE-cad, VEGFR-2, and ICAM2. (A) Importantly, a 1 mg/kg total dose consisted of 0.075 mg/kg siVE-cad, 0.125 mg/kg siICAM2, 0.25 mg/kg siVEGFR-2, 0.25 mg/kg siTie2, and 0.30 mg/kg siTie1.

a

Legend:
- 0.30 Tie1
- 0.25 Tie2
- 0.25 VEGFR-2
- 0.08 VE-cad
- 0.13 ICAM-2

b

Total Dose (mg/kg)	2.0 siLuc	1.5 si 5 genes	1.0 si 5 genes	0.5 si 5 genes	0.25 si 5 genes
Tie1	1.02 ± 0.16	0.15 ± 0.02	0.22 ± 0.05	0.33 ± 0.08	0.60 ± 0.06
Tie2	0.90 ± 0.08	0.37 ± 0.02	0.43 ± 0.02	0.38 ± 0.04	0.56 ± 0.03
VE-cad	0.88 ± 0.18	0.26 ± 0.01	0.31 ± 0.07	0.49 ± 0.13	0.75 ± 0.09
VEGFR-2	0.99 ± 0.13	0.22 ± 0.03	0.23 ± 0.03	0.41 ± 0.09	0.65 ± 0.04
ICAM2	1.15 ± 0.26	0.24 ± 0.04	0.34 ± 0.09	0.65 ± 0.28	1.13 ± 0.14

c

Total Dose (mg/kg)	2.0 siLuc	1.5 si 5 genes	1.0 si 5 genes	0.5 si 5 genes	0.25 si 5 genes
Tie1	1.22 ± 0.15	0.25 ± 0.03	0.31 ± 0.04	0.48 ± 0.08	0.87 ± 0.11
Tie2	1.35 ± 0.19	0.31 ± 0.04	0.32 ± 0.03	0.48 ± 0.09	0.92 ± 0.09
VE-cad	0.92 ± 0.06	0.49 ± 0.16	0.67 ± 0.03	0.73 ± 0.14	1.19 ± 0.07
VEGFR-2	1.46 ± 0.27	0.32 ± 0.08	0.54 ± 0.09	0.93 ± 0.14	0.93 ± 0.13
ICAM2	1.24 ± 0.24	0.54 ± 0.11	0.65 ± 0.08	0.89 ± 0.14	1.23 ± 0.07

d

Total Dose (mg/kg)	2.0 siLuc	1.5 si 5 genes	1.0 si 5 genes	0.5 si 5 genes	0.25 si 5 genes
Tie1	1.15 ± 0.20	0.65 ± 0.12	0.78 ± 0.12	0.89 ± 0.15	0.84 ± 0.15
Tie2	0.92 ± 0.15	0.56 ± 0.12	0.80 ± 0.10	0.79 ± 0.04	0.67 ± 0.23
VE-cad	1.17 ± 0.48	0.77 ± 0.11	0.98 ± 0.22	0.96 ± 0.14	0.85 ± 0.22
VEGFR-2	0.90 ± 0.20	0.81 ± 0.10	0.95 ± 0.20	0.88 ± 0.10	0.86 ± 0.15
ICAM2	1.15 ± 0.33	1.08 ± 0.13	1.42 ± 0.22	1.07 ± 0.09	0.93 ± 0.10